Available online at www.sciencedirect.com
SCIENCE DIRECT®
Journal of the European Ceramic Society 25 (2005) 1499–1506
www.elsevier.com/locate/jeurceramsoc

Alumina-rich refractory concretes with added spinel, periclase and dolomite: A comparative study of their microstructural evolution with temperature

L.A. Díaz[a], R. Torrecillas[a,*], A.H. De Aza[b], P. Pena[b], S. De Aza[b]

[a] *Department of Chemistry of Materials, Instituto Nacional del Carbón-CSIC, C/Francisco Pintado Fe, 26, La Corredoria, 33011 Oviedo, Spain*
[b] *Instituto de Cerámica y Vidrio, CSIC, Campus de Cantoblanco, Camino de Valdelatas, s/n, 28049 Madrid, Spain*

Received 25 October 2003; received in revised form 26 May 2004; accepted 31 May 2004
Available online 12 August 2004

Abstract

Three processing routes for obtaining refractory castables within the alumina-rich zone of the Al_2O_3–MgO–CaO ternary phase equilibrium diagram were studied starting from mixtures of: (a) calcined alumina, synthetic spinel and calcium aluminate cements, (b) calcined alumina, magnesia and calcium aluminate cement, and (c) calcined alumina, dolomite and calcium aluminate cement. The evolution of the phases and microstructure was studied as a function of temperature and the processing route for both refractory concretes and their corresponding matrices (<125 μm).

Keywords: Refractories; Castables; Al_2O_3; $MgAl_2O_4$; MgO; Dolomite; Phase evolution; Microstructure

1. Introduction

Intensive R&D carried out in recent years in the field of refractory concretes (for the metallurgical sector) has led to a considerable increase in their use as linings for secondary steel plant ladles. The presence of magnesium spinel in the composition of alumina-rich refractory concretes has clearly improved slag attack behaviour, reduced wear rates[1–4] and as a consequence provided a longer lifespan for steel plant ladles than other traditional refractory products.

Now magnesia (dead burned magnesite) is used as an additive as a means of generating "in situ spinel" by reactive sintering, resulting in an even greater resistance to corrosion and slag penetration in comparison with high alumina concretes with added synthetic spinel. However, the use of magnesia presents certain disadvantages due to hydration and other associated rheological problems.[5–12] The use of dolomite as an additive in refractory concretes has not been widely reported in the literature. The composition of the alumina-rich refractory concretes with added spinel, magnesia or dolomite, which are currently employed in the steel industry is located within the alumina-rich corner of the Al_2O_3–MgO–CaO ternary phase equilibrium diagram. The designing of materials in the high alumina zone within this ternary system has two significant advantages:

(a) The presence of high invariant points with temperatures generally above 1700 °C makes it possible to design materials with a high refractoriness.
(b) Due to the broad primary crystallisation field of spinel ($MgAl_2O_3$) in many oxide systems, the designed concretes will show low solubility against molten products. Additionally, spinel is a crystalline phase that absorbs a large amount of metal cations (Fe^{3+}, Fe^{2+}, Mn^{2+}, etc.) into its structure, forming a wide range of solid solutions.

In this research work, three processing routes for obtaining refractory concretes within the alumina-rich zone of the Al_2O_3–MgO–CaO ternary system were studied. In all of

* Corresponding author.
E-mail addresses: ladiaz@incar.csic.es (L.A. Díaz), rtorre@incar.csic.es (R. Torrecillas).

0955-2219/$ – see front matter © 2004 Elsevier Ltd. All rights reserved.
doi:10.1016/j.jeurceramsoc.2004.05.018

Table 1
Particle size results of the finer raw materials used to obtain refractory castables (results in vol.%)

Raw materials	<2 μm	2–4 μm	4–8 μm	8–16 μm	16–32 μm	32–62 μm	>62 μm
CT9SG	25.54	18.75	27.57	22.03	5.42	0.63	0.06
CL370C	58.73	17.46	20.52	3.29			
AR78	34.64	18.74	26.43	19.70	0.49		
CA270	31.14	19.76	21.32	13.77	7.53	3.76	2.72
Magnesia	39.10	12.54	15.76	17.83	10.15	3.07	1.55
Dolomite	30.33	18.56	24.01	21.53	5.43	0.14	

these materials large and medium grains of tabular alumina and white corundum were used, whereas the finest grains (fractions smaller than 125 μm) were made up of the following mixtures:

(1) Calcined alumina, synthetic spinel and calcium aluminate cement.
(2) Calcined alumina, magnesia and calcium aluminate cement.
(3) Calcined alumina, dolomite and calcium aluminate cement.

The evolution of the phases and microstructure as a function of temperature was studied for the different processing routes both in the refractory concretes and in their corresponding matrices.

2. Experimental methodology

2.1. Design of the compositions

The key to designing both shaped and monolithic refractory materials with excellent behaviour against molten slags lies in the appropriate selection of the components present in the finer fractions, i.e. amount, grain size, chemical composition, etc.

Of the possible combinations of raw materials for the processing of refractory concretes in the alumina rich zone of the Al_2O_3–MgO–CaO ternary diagram, the following were used: tabular alumina (T-60, -14 mesh and 6–10 mesh) (Alcoa, Germany), calcined aluminas (CT9SG and CL370C) (Alcoa, Germany), synthetic spinel (AR78) and calcium aluminate cement (CA270) (Alcoa, Germany), white corundum (0–0.2 mm and 0.2–2 mm) (Pechiney, France); sintered magnesium oxide (CF Grade) (Dead Sea Periclase Ltd., Israel); and dolomite (Prodomasa, Spain). Darvan 7S (organic polyacrylate polymer) was used in concentrations of 0.03 wt.% as an additive to control the rheological behaviour of the concretes. Table 1 presents a granulometric analysis of the finest fractions (<125 μm).

Two basic factors were taken into consideration in designing the composition:[13] (a) chemical composition and (b) grain size.

2.1.1. Chemical composition

Table 2 contains the chemical compositions of the different matrices of the selected concretes. All the raw material mixtures were chosen so that at high temperatures (1650 °C) the materials would have the same spinel content in the matrix. Spinel contents of 5, 10, 15 and 20 wt.% were studied, and their corresponding compositions were named 8D5%, 8D10%, 8D15% and 8D20%. In the case of materials made from the addition of magnesia, calculations were carried out so that final spinel contents of 5, 10, 15 and 20 wt.% would be obtained at high temperatures (1650 °C) once equilibrium had been reached. These compositions were named 8DM5%, 8DM10%, 8DM15% and 8DM20%. In the case of dolomite additions, the compositions were labelled PKDOL5%, PKDOL10%, PKDOL15% and PKDOL20%. In this case, only PKDOL5% has the same final spinel content as 8D5% and 8DM5%, the others having similar magnesia contents to those of Fig. 1, where all the compositions designed have been located inside the ternary phase equilibrium diagram. The calcium aluminate cement content was kept constant for all compositions (8 wt.%), except for those prepared with dolomite, where 2 wt.% was used for PKDOL5% and PKDOL10% and 1.5 wt.% for compositions PKDOL15% and PKDOL20%.

Table 2
X-ray fluorescence analysis of raw materials (results in wt.%)

Raw materials	Al_2O_3	SiO_2	Fe_2O_3	TiO_2	CaO	MgO	Na_2O	K_2O	P_2O_5	LOI
CT9SG	99.18	0.33	0.03	0.15	0.05	0.13	0.08		0.03	0.01
CL370C	99.8	0.03	0.03		0.02		0.06			
AR78	77.1	0.05	0.08		0.25	22.4	0.13			
CA270	73.5	0.2	0.07		25.9	0.1	0.20			0.02
Magnesia	0.02	0.03	0.03		0.52	99.3				
Dolomite	0.011	0.018	0.008		30.27	22.05				47.7

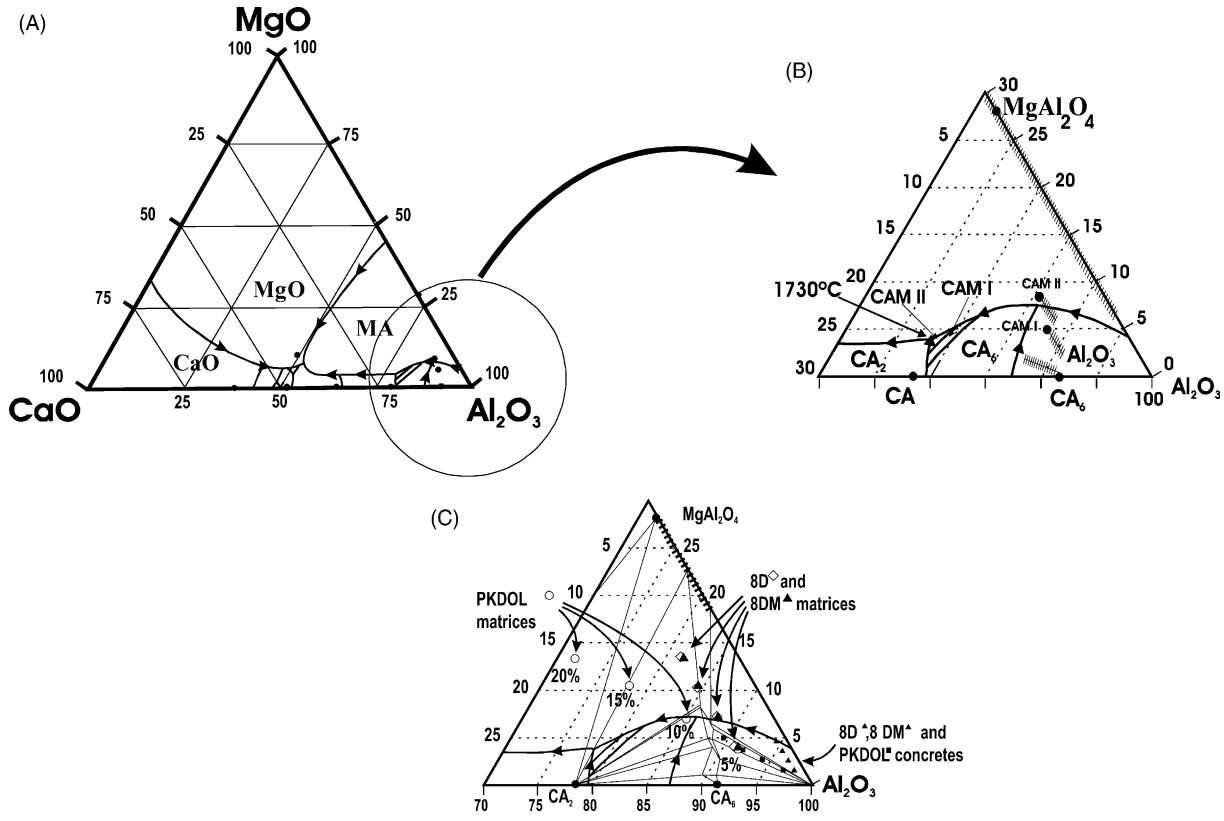

Fig. 1. (A) Al_2O_3–MgO–CaO ternary phase equilibrium diagram, (B) alumina-rich zone, and (C) location of all the designed compositions in the alumina rich zone.

2.1.2. Grain size

So that the granulometric curve would be the same for all the concretes obtained by the different processing routes it was necessary to develop a software which would allow us to calculate the chemical composition of the refractory concretes and that of the corresponding matrices (fraction, <125 μm). The total granulometric curve was also calculated from the percentages of the raw materials used. The software was based on Andeassen's equation and follows a "gap-sized" granulometric curve.[14]

2.2. Processing

First the mixtures were dry-mixed in a mixer (Prat®). Subsequently water was progressively added (ratio water/cement = 0.9), while the total mixture was subjected to continuous stirring for 3 min. The corresponding matrices of the refractory concretes were obtained by sieving the starting raw material mixtures down to 125 μm. The powders obtained were mixed at water/cement ratios of between 1.75 and 2.13. The fluidity of the elaborated concretes was studied following the ASTM C230-90 Standard. All the samples were cured at room temperature in airtight containers for 24 h and then dried at 110 °C for 24 h before being subjected to the corresponding thermal treatments. The castables obtained were poured into metal moulds with the following dimensions: 25 mm × 25 mm × 150 mm. The refractory concretes were subjected to thermal treatments from 400 to 1750 °C. The heating rate from room temperature to 980 °C was 330 °C/h and from then on to the final temperature the rate was 110 °C/h. The samples were held at the maximum temperature for 12 h. The matrix samples were subjected to the same thermal treatment but they were held at the maximum temperature for 2 h.

Phase evolution as a function of temperature was studied by X-ray diffraction (Siemens D-5000, employing Cu radiation and operating at 30 mA and 40 kV). The samples were ground and sieved down to 40 μm after being subjected to the different thermal treatements. A semi-quantitative analysis taking into account the integrated area of the peak intensity obtained by XRD was also carried out.

The microstructure of the fired samples (matrices and concretes) was examined both in the case of the polished samples (concretes) and in the case of the fracture surfaces (matrices) by scanning electron microscopy (SEM) (Zeiss, DSM-942) equipped with EDX (Oxford Link Isis II EDS). All the samples were coated with a thin layer of gold.

Dynamic sintering studies up to 1650 °C at a heating rate of 5 °C/min were carried out for concretes and their matrices using a Netsch 402E dilatometer in air.

3. Results and discussion

3.1. Microstructure and phase evolution with temperature

The changes in microstructure and phase evolution during the first stages of sintering were mainly due to the calcium aluminate transformations, whereas at higher temperatures the change in evolution was clearly due to alumina/magnesia and alumina/dolomite reactions. Fig. 2a and b show the microstructure of composition 8D10% after the thermal treatment at 1650 °C.

At low temperatures (110 °C) the phases present in the concretes are: alumina gel, traces of calcium aluminate cement hydrates (C_3AH_6 and CAH_{10}) and calcined alumina, as well as magnesia and dolomite, depending on the type of concrete. Phase evolution with temperature from 400 to 1750 °C can easily be followed in the case of the concrete matrices. The phases observed and their evolution are as follows:

$C_{12}A_7$: This phase becomes noticeable at 600 °C in all the matrices of the 8D compositions due to the dehydration of the stable hydrates of the calcium aluminate cement. Its degree of crystallinity gradually increases until it reaches a maximum value in the 800–1000 °C range. At 1100 °C this phase cannot be detected by XRD. Examination of the fracture surface of the matrices by scanning electron microscopy shows that $C_{12}A_7$ posesses the pseudomorphic appearance of the hydrates from which it originates, with laminar, prismatic growth and a cubic structure (Fig. 3). In the case of matrices corresponding to compositions containing magnesia, the maximum degree of recrystallisation occurs at lower temperatures (600–800 °C).

CA: This phase appears as traces from 800 °C onwards due to the reaction $C_{12}A_7 + A \rightarrow CA$. The maximum degree of recrystallisation is reached at 1000 °C and from this temperature onwards CA gradually reacts with the alumina to form CA_2. At 1400 °C, CA is no longer visible. It presents a globular morphology (Fig. 4). In the case of the compositions formed with dolomite (PKDOL5%, PKDOL10% and PKDOL15%), the CA phase is undetectable at 1200 °C. In the case of the PKDOL20% the CA is also undetectable from 1400 °C onwards, because this composition is located inside the $CA–CA_2–AM_{ss}$ compatibility triangle (see Fig. 1), where the CA phase is not stable.

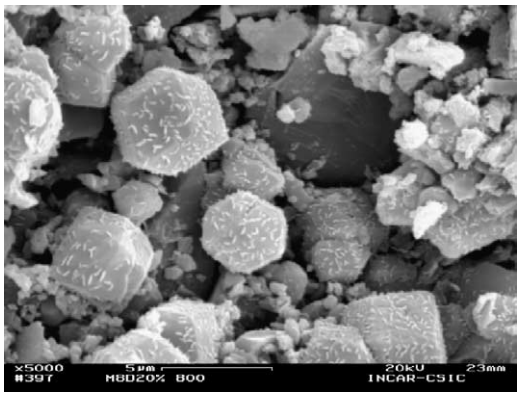

Fig. 3. $C_{12}A_7$ crystals with a cubic morphology and several microcrystals that have precipitated onto their surface (800 °C).

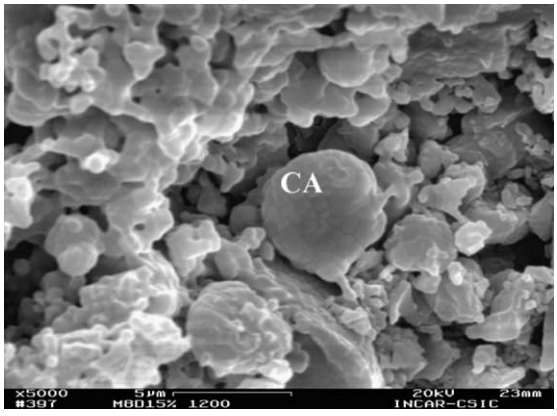

Fig. 4. CA crystal with a globular morphology (1200 °C).

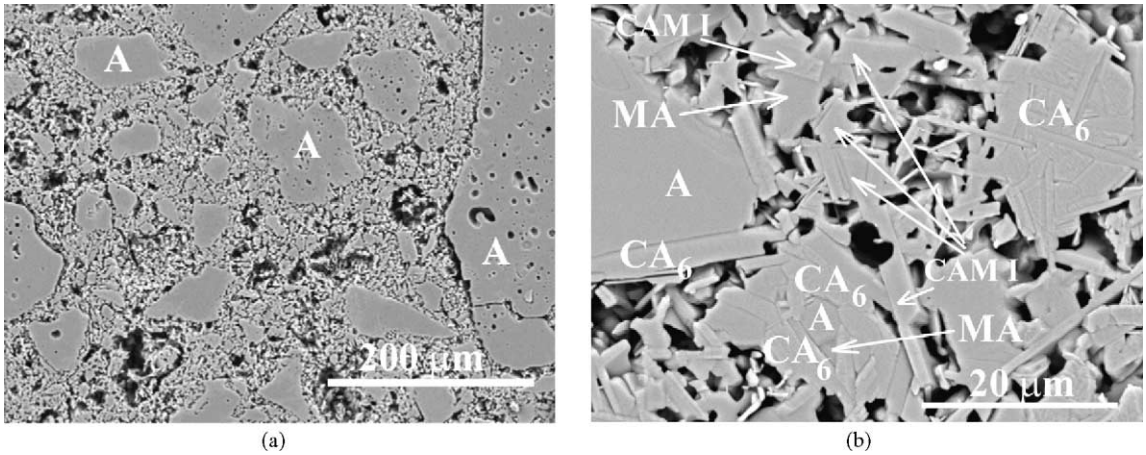

Fig. 2. (a) SEM microstructure of the 8D10% refractory castable (1650 °C). (b) Detailed view of the previous SEM micrograph (1650 °C). A, alumina; MA, spinel.

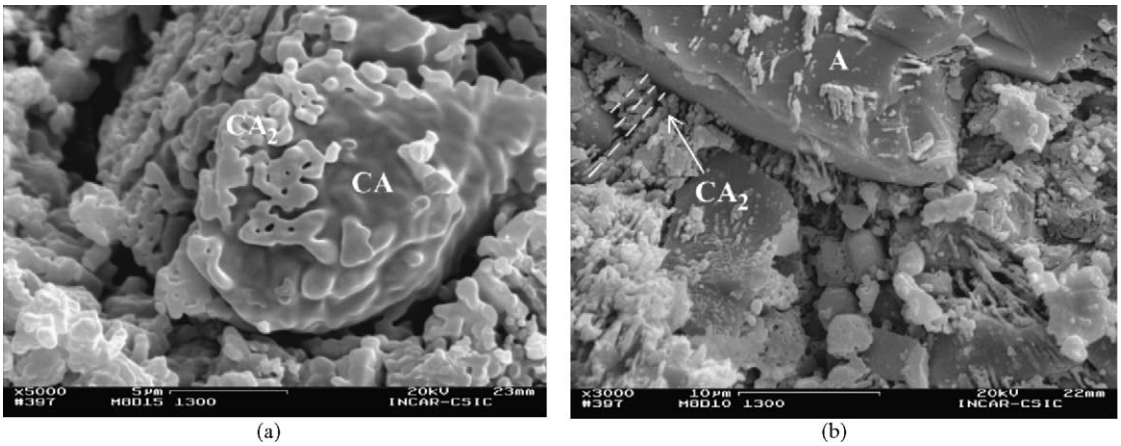

Fig. 5. (a) Intergrowth of CA and CA_2 crystals with vitreous phase (1300 °C). (b) Perpendicular orientation of CA_2 crystals towards the white corundum crystal (A) at 1300 °C.

CA_2: The formation of this phase from CA and alumina is associated with a 13.6% volume increase which becomes perceptible above 1000 °C. The formation of a glassy phase at about 1300 °C (see Fig. 5a) allows part of the alumina and CA to dissolve, precipitating CA_2. Up to temperatures close to 1300 °C, its morphological appearance under SEM is of the tabular type or one of oriented microcrystals that tend to become alligned perpendicularly to the white corundum crystals existing inside the matrix (Fig. 5b). In the matrices corresponding to the 8D15% and 8D20% compositions, CA_2 can be detected once the samples have been subjected to a temperature of 1700 °C, whereas this does not occur in the case of the matrices corresponding to the 8D5% and 8D10% compositions which were also subjected to this temperature. This inconsistency is due to the fact that the compositions occupy different locations within the ternary phase equilibrium diagram. Thus, the compositions with 15% and 20 wt.% of synthetic spinel in the matrix are located within the CA_2–AM_{ss}–$CAMI_{ss}$ compatibility triangle; whereas the other two compositions (5% and 10%) are located within the AM_{ss}–$CAMII_{ss}$–A compatibility triangle, where CA_2 is not a stable phase. The compositions with magnesia present a CA_2 phase evolution similar to that described above. For the PKDOL5% and PKDOL10% compositions, CA_2 is detected between 1100 °C and 1400 °C, whereas in the compositions with 15% and 20% dolomite, CA_2 is detected above 1600 °C and 1700 °C, respectively.

CA_6: This phase appears from 1400 °C onwards. Its maximum degree of crystallisation takes place at 1600 °C and from there onwards it begins to react with spinel to form the CAMI and CAMII ternary compounds. The CA_6 crystals have a morphology of interwoven platelets (Fig. 6) and a reaction aureole is formed around the corundum crystals. Of the prepared matrices, the 5% compositions show the highest CA_6 content at 1600 °C, due to their close proximity to CA_6 within the AM_{ss}–CA_6–A compatibility triangle. In the case of the PKDOL20% matrix composition the CA_6 phase cannot be detected by X-ray diffraction at 1750 °C.

MA ($MgAl_2O_4$): Spinel is a stable phase at high temperatures as the compositions are located within its primary crystallisation field, with the exception of the 5% compositions (see Fig. 1). When the temperature is increased, alumina is introduced as a solid solution inside the structure of the spinel. As a result the X-ray diffraction peaks shift towards higher 2θ angles.[15,16] In the case of the compositions prepared with magnesia, spinel is formed at 1200 °C by reaction of magnesia and alumina. The evolution of the amount of spinel with temperature presents two maximums, one in the 1200–1300 °C range and a second maximum between 1500 and 1600 °C. The second maximum shows a higher value than the former, which may be related with the coarse grain size of the magnesia used in the preparation of materials. It should be pointed out that the temperature must be raised for the reactions to be completed (total reaction of magnesia). The size of the spinel crystals obtained by sintering reactions (8DM compositions) is finer than the crystal size of the added synthetic spinel (8D compositions) (Fig. 7). In the case of the compositions made with dolomite, spinel does not appear in such quantities due to the different locations of the compositions within the Al_2O_3–MgO–CaO ternary system. Spinel appears

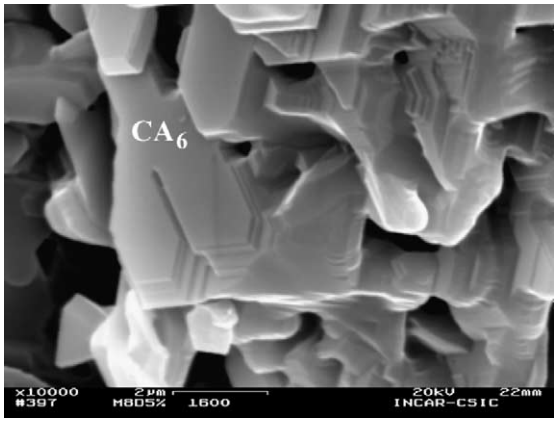

Fig. 6. CA6 platelets at 1600 °C in the 8D5% matrix composition.

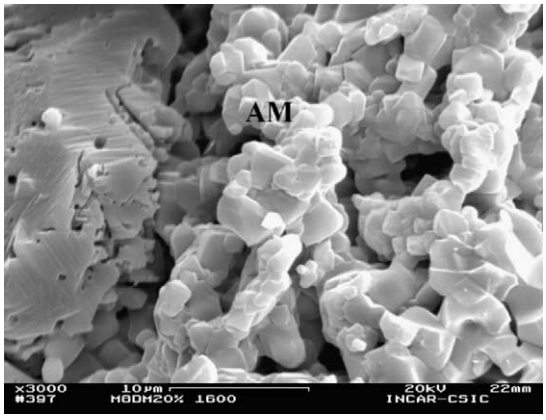

Fig. 7. Spinel crystals (AM) in the 8DM20% matrix composition at 1600 °C.

from 1100 °C onwards; its greatest degree of crystallisation is observed between 1200 and 1300 °C in the 5% and 10% compositions. For the PKDOL15% and PKDOL20% matrices, spinel is a stable phase, even at temperatures as high as 1750 °C, whereas it disappears at this temperature for the remaining matrices. It has a very fine grain size.

Alumina (α-Al_2O_3): The concentration of alumina starts to decrease above 1000 °C due to the series of reactions with the calcium aluminate cement phases ($C_{12}A_7$, CA and CA_2) up to 1200 °C. At 1300 °C, the alumina begins to react with CA_2 to form CA_6. In the 5% and 10% compositions, there is an increase in the alumina content at 1700 °C, whereas alumina is not present in the 15% and 20% compositions because it is not a stable phase at this temperature.

CAMI ($CaMg_2Al_{28}O_{46}$) and CAMII ($CaMg_2Al_{16}O_{27}$): These two new phases were first reported by Göbbels et al.[17] and Iyi et al.[18] and are located on the line that connects CA_6 and the stoichiometric spinel. They are made up of a laminar structure derived from CA_6, which is isostructural with the structure of magnetoplumbite, but with much larger dimensions along the *c* axis. They possess a 3rd-order crystallographic axis with two structural blocks: one denominated S with an AM composition, and another denominated M, with a CA_6 composition. Therefore both compounds may be considered as two different structures with different block-piling sequences: $(M_2S)_n$ in the case of CAMI (*c* = 79.77 Å) and $(MS)_n$ in the case of CAMII (*c* = 31.297 Å). These two compounds are polytypoidal,[19] since they present variations in composition as a result of the periodical changes in the block piling sequence that gives form to their structure.

The CAMI phase was detected up to 1750 °C in the 8D5%, 8D10%, 8D15% and 8D20% compositions; whereas the CAMII phase was only detected at 1750 °C in the 8D15% and 8D20% compositions. Fig. 8a and b show the morphological character of their crystallisation. In the case of the matrices prepared with magnesia, the CAMI phase was detected in the 1700–1750 °C range in all the compositions. However, only the composition of the 8DM20% matrix presents the CAMII phase at 1750 °C. As regards the compositions made with dolomite, both the CAMI and CAMII phases are observed at 1700 °C, except for composition PKDOL5%. At 1750 °C, composition PKDOL20% only presents the CAMII phase.

Periclase (MgO): This phase is observed in all the compositions of the 8DM type up to 1400 °C. It is not detected at 1500 °C, its disappearance coinciding with the maximum value of spinel crystallisation. In the compositions made with dolomite, magnesia is only observed between 800 and 1000 °C for the 15% and 20% compositions, due to the decomposition of the dolomite. In these compositions, the magnesia disappears at 1200 °C as it reacts with alumina to form spinel.

Dolomite [$Mg,Ca(CO_3)_2$]: This phase constitutes the raw material of the PKDOL-type matrices and it remains present unless it decomposes at 600 °C for the PKDOL15% and PKDOL20% compositions and 800 °C for the PKDOL5% and PKDOL10% compositions.

Calcite ($CaCO_3$): This is a metastable phase which can be detected in the compositions made with dolomite in the 600–800 °C range.

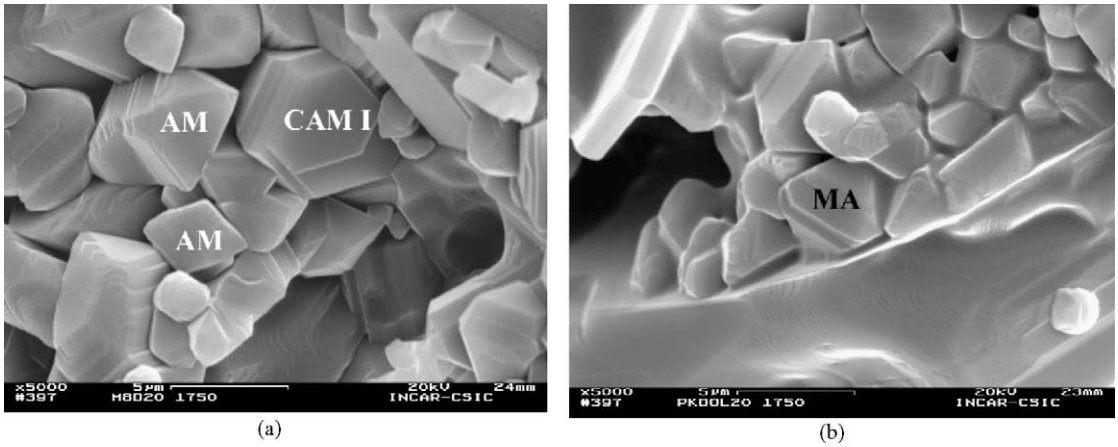

Fig. 8. (a) Spinel crystals (AM) and CAMI compounds at 1750 °C. (b) Spinel crystals coexisting with CAMII compounds (lower part of the micrograph) (PKDOL20% matrix).

Calcia (CaO): This was only detected in the PKDOL15% and PKDOL20% matrices in the 600–800 °C range, due to the decomposition of the dolomite.

3.2. Dynamic sintering curves

Several dynamic sintering curves were obtained using cured test specimens for the different concretes and matrices designed. After the dilatometric measurements were completed, structural changes could best be appreciated in the case of the matrices (Fig. 9). In all of these tests, a slight expansion can be appreciated up to approximately 150 °C which may be attributed to the process of conversion of the metastable hydrates to stable hydrates. From 200 to 300 °C, there is a marked contraction due to the dehydration process of the stable hydrate C_3AH_6 (katoite), as a result of which decohesion takes place between the large grains of the concrete and the matrix, giving rise to an internal network of microcracks within the sample. Above 1100 °C, the curves present a different expansion behaviour depending on the type of matrix under study. In the light of the XRD results, the expansion can be ascribed to the formation of the CA and CA_2 phases. After that, a significant contraction takes place between 1250 and 1400 °C, due to sintering in the presence of a transitory liquid phase (disappearance of CA), up to approximately 1480 °C, at which temperature there is a pronounced expansion, except in the case of the 8D20% sample due to the formation of the CA_6 phase. Once again, from 1600 °C onwards, a slight shrinkage is observed as a result of sintering until 1650 °C is reached. Up to 1000 °C the cooling curves manifest a fairly linear behaviour and are all practically parallel. The behaviour of the dynamic sintering curve of the composition corresponding to the matrix of 8D5% differs from the other compositions in that it is located within a different compatibility triangle, i.e. within the $CAMI_{ss}$–$CAMII_{ss}$–A compatibility triangle, in which spinel is not a stable phase.

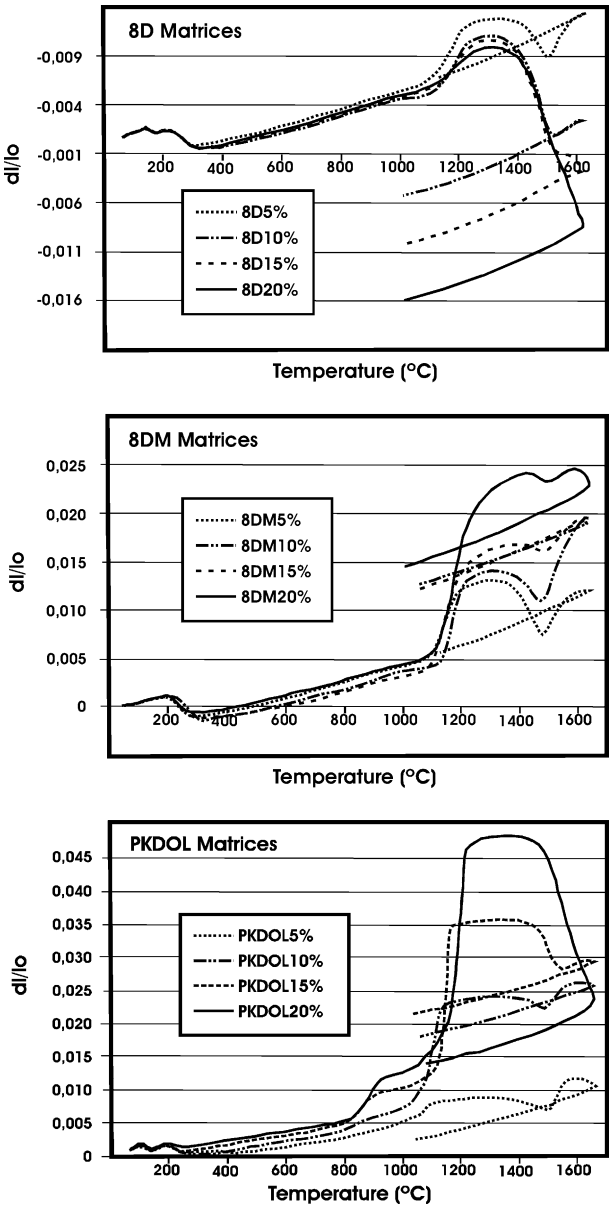

Fig. 9. Dynamic sintering curves from all the matrices tested.

The results corresponding to the thermal expansion of the matrices prepared with magnesium (8DM) are fairly similar to those of the compositions made with synthetic spinel (8D), except for the formation of the spinel phase around 1100 °C. Considerable expansion takes place from 1080 °C onwards, due to the formation of CA_2 and the commencement of spinel crystallisation. This expansion is proportional to the magnesia content in the compositions.

The dynamic sintering curves of the PKDOL matrices present a significant expansion from 800 °C onwards, due to the decomposition of the dolomite and the crystallisation of the CA phase. Another significant expansion is appreciated around 1050 °C, due firstly to the crystallisation of the CA_2 and subsequently to the formation of spinel. This expansion is also proportional to the amount of dolomite added to the matrices. In the 1450–1480 °C range, the expansion of the matrices due to the formation of CA_6 gradually decreases as a function of the dolomite content. This behaviour is in agreement with that observed previously for the 8D and 8DM matrices as, with the increase in synthetic spinel, magnesia or dolomite contents within the matrix, the location of the compositions moves away from the CA_6 phase.

4. Conclusions

The evolution of the phases with temperature corresponding to the materials designed is determined by the series of reactions that take place between the alumina and calcium aluminate cement phases. The $C_{12}A_7$ phase appears from 600 °C onwards, its highest degree of crystallisation being observed at a lower temperature in the compositions formed with magnesia and dolomite as compared to those made with synthetic spinel (8D). The CA phase appears as traces from 800 °C onwards, its highest degree of crystallisation being

observed at around 1000 °C. Above this temperature, the CA reacts with the alumina and thereby initiates the formation of the CA_2 phase. This phase is very expansive, especially after 1100 °C, as any deformation is absorbed into the material due to the significant amount of liquid phase present at this temperature. The CA_6 phase becomes apparent at 1400 °C with a morphology of small, interwoven platelets, while above 1650 °C, it reacts with spinel to form the CAMI and CAMII ternary phases. As for the compositions made with dolomite and magnesia, spinel is formed due to sintering reactions with alumina above the temperatures of 1100 and 1200 °C, respectively. Spinel is a stable phase at high temperatures, except in the 5% compositions. The grain size of the self-forming spinels (compositions 8DM and PKDOL) is much finer than the crystal size of the added synthetic spinel (type 8D compositions).

Acknowledgement

The authors wish to thank the EU for its support under a Brite Euram Project, under Contract No. BRPR-CT 97-0427.

References

[1] Sato, Y., Joguchi, H. and Hiroki, N., Test results of alumina-spinel castables for steel ladle. *Taikabutsu Overseas*, 1992, **12**(1), 10–14.
[2] Mori, J., Onove, M., Toritani, Y. and Tanaka, S., Structure change of alumina castable by addition of magnesia or spinel. *Taikabutsu Overseas*, 1995, **15**(3), 20–23.
[3] Isobe, T., Matsumoto, O., Itose, S., Kawano, F., Saihi, K., Takiuchi, S. and Oda, Y., Sinterability of spinel raw fine powder and application to castables. *Taikabutsu Overseas*, 1995, **15**(3), 10–13.
[4] Shima, K., Imaiida, Y. and Katani, T., Application of alumina-spinel castable to teeming ladle for stainless steel. *Taikabutsu Overseas*, 1995, **15**(3), 24–28.
[5] Brandao, P., Goncalves, G. E. and Duarte, A. K., Mechanisms of hydration/carbonation of basic refractories. *Refract. Appl.*, 1998, **3**(2), 6–8.
[6] Brandao, P., Goncalves, G. E. and Duarte, A. K., Mechanisms of hydration/carbonation of basic refractories. Part 2. Investigation of the kinetics of formation of brucite in fired basic bricks. *Refract. Appl.*, 1998, **3**(2), 9–11.
[7] Kaneyasu, A., Yamamoto, S. and Yoshida, A., Magnesia raw materials with improved hydration resistance. *Taikabutsu Overseas*, 1997, **17**(2), 21–26.
[8] Kaneyasu, A., Arita, Y., Yoshida, A. and Watanabe, T., Hydration resistance of MgO aggregate with added CaO. *Taikabutsu Overseas*, 1999, **19**(1), 30–34.
[9] Kaneyasu, A., Yamamoto, S. and Watanabe, T., MgO raw material with improved hydration resistance. *Taikabutsu Overseas*, 1996, **16**(2), 26–30.
[10] Kitamura, A., Onizuka, K. and Tanaka, K., Hydration characteristics of magnesia. *Taikabutsu Overseas*, 1996, **16**(3), 3–11.
[11] Koga, Y., Sato, M., Sekiguchi, K. and Iwamoto, S., Effects of alumina cement grade and additives on alumina-magnesia castables containing aluminum lactate. *Taikabutsu Overseas*, 1998, **18**(1), 43–47.
[12] Malarria, J. A. and Tinivella, R., Degradation of refractory brick by hydration. *Am. Ceram. Soc. Bull.*, 1998, 69–73.
[13] Díaz, L. A., *Materiales refractarios monolíticos de alta alúmina dentro del sistema Al_2O_3–MgO–CaO*. Ph.D. thesis, Universidad Autónoma de Madrid, Spain, 2000, p. 238.
[14] Myhre, B., Particle size distribution and its relevance in refractory castables. In *The 2nd India International Refractory Congress, New Delhi, 8th–9th February, 1996. Vol 7*, 7 pp.
[15] Fuhrer, M., Hey, A. and Lee, W. E., Microstructural evolution in self-forming spinel/calcium aluminated-bonded castables refractories. *J. Eur. Ceram. Soc.*, 1998, **18**, 813–820.
[16] Cisar, A., Henslee, W. W. and Strother, G. W., Development of spinel-bases specialities: mortars to monoliths. In *Advances in Ceramics, New Developments in Monolithic Refractories, Vol 13*, ed. E. F. Robert. The American Ceramic Society , 1985, pp. 411–418.
[17] Göbbels, M., Woermann, E. and Jung, J., The Al-rich part of the system CaO–Al_2O_3–MgO. Part I. Phase relationships. *J. Solid State Chem.*, 1995, **120**, 358–363.
[18] Iyi, N., Göbbels, M. and Matsui, Y., The Al-rich part of the system CaO–Al_2O_3–MgO. Part II. Structure refinement of two new magnetoplumbite-related phases. *J. Solid State Chem.*, 1995, **120**, 364–371.
[19] De Aza, A. H., Iglesias, J. E., Pena, P. and De Aza, S., Ternary system Al_2O_3–MgO–CaO. Part II. Phase relationships in the subsystem Al_2O_3–$MgAl_2O_4$–$CaAl_4O_7$. *J. Am. Ceram. Soc.*, 2000, **83**(4), 919–927.